Materials Science in Semiconductor Processing 74 (2018) 88–97

Contents lists available at ScienceDirect

Materials Science in Semiconductor Processing

journal homepage: www.elsevier.com/locate/mssp

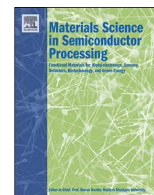

Electrical isolation of GaAs and AlGaAs/GaAs Quantum Cascade Lasers by deep hydrogen implantation

Maciej Artur Kozubal[a,*], Anna Szerling[a], Kamil Kosiel[a], Marcin Myśliwiec[b], Karolina Pągowska[a], Rafał Jakieła[c], Renata Kruszka[a], Marek Guziewicz[a], Adam Barcz[a,c]

[a] Department of Micro- and Nanotechnology of Wide Bandgap Semiconductors, Institute of Electron Technology, Al. Lotników 32/46, 02-668 Warsaw, Poland
[b] Insititute of Microelectronics and Optoelectronics, Warsaw University of Technology, Nowowiejska 15/19, 00-665 Warsaw, Poland
[c] Institute of Physics, Polish Academy of Sciences, Al. Lotników 32/46, 02-668 Warsaw, Poland

ARTICLE INFO

Keywords:
Hydrogen implantation
Electrical isolation
GaAs
AlGaAs/GaAs
Quantum Cascade Laser
RBS/c

ABSTRACT

Ion implantation can be applied to form the electrical isolation in AlGaAs/GaAs Quantum Cascade Laser (QCL) instead of mesa etching. In this paper, we present in detail the designing of hydrogen implant isolation scheme, alongside with its verification and study of thermal stability by structural and electrical characterization techniques. Our scheme employed 4 µm thick metallic mask made mainly of gold which also served as contact layer, and 640 keV hydrogen implantation to a fluency of 1×10^{15} cm^{-2}. We obtained the sheet resistivity R_{SH} of $(1.5 \pm 0.9) \times 10^9$ Ω/□. The critical temperature for the hydrogen implant isolation fabrication of the AlGaAs/GaAs QCL was determined to be 310 °C. Defect density dropped to residual levels after 1 min annealing at 300 °C and 400 °C, while the material was still resistive with R_{SH} above 10^8 Ω/□. Based on our simulated vacancy maps we concluded that the minimum width of the masking structure should be at least 5 µm to avoid the effects of lateral isolation for the given implantation conditions. The QCL device fabricated with this isolation scheme operated with threshold current densities of 6 kA/cm^2 at the temperature of 77 K. Ultimately, we confirmed the applicability of hydrogen implant isolation for the manufacturing of optical devices.

1. Introduction

Quantum Cascade Laser is an unipolar device with periodic semiconductor structure, where electrons undergoing intersubband transitions emit photons, then tunnel to the next period [1]. They are excellent sources of mid- and far-infrared laser radiation, MIR ($\gtrsim$ 2.6 µm) and FIR ($\lesssim$ 250 µm), respectively. For these applications GaAs/AlGaAs heterostructures are commonly used among other III-V material systems [2,3]. QCLs are used in gas-sensing applications, infrared spectrometry, medical diagnostics, environmental monitoring etc.

Ion implantation in III-V compounds is commonly employed in the manufacturing of semiconductor devices and integrated circuits (ICs) [4–6]. It is used for dopant introduction and for electrical isolation. In the latter process, called implantation-isolation, defects produced act as traps for carriers converting the conducting regions into highly resistive ones.

Defect formation and electrical isolation resulting from ion implantation in GaAs has been studied [7,8] especially regarding the ion mass, dose and annealing temperature [9–11]. In GaAs-based Quantum Cascade Lasers with mesa structure the shallow ion implantation was employed instead of dielectric isolation layers [12–15]. The same approach was used for GaInAs/AlInAs heterostructure [16]. The proton irradiation was also applied for a passive waveguide fabrication in GaInAs/AlInAs [17]. Similarly, deep electrical isolation by ion implantation was introduced into the Terahertz Quantum Cascade Laser (THz QCL) [18,19].

In this work we presented the design process and verification of scheme for deep electrical isolation of AlGaAs/GaAs quantum cascade laser by high energy proton implantation. Our previous publication on this topic concerned the final isolation scheme as applied to the mid-infrared (~ 9.5 µm) $Al_{0.45}Ga_{0.55}As$/GaAs plasmon-enhanced-waveguide quantum-cascade laser [20]. This work elaborates in detail on the planning steps, presenting the line of thought that allowed to establish the proper parameters. We expanded on theoretical simulations, including unique calculations of vacancy maps. Structural and electrical measurements were carried out in order to verify the atom and vacancy profiles as well as the fabricated isolation. Furthermore, series of experiments was performed in order to determine thermal stability of the implantation isolation and to specify the maximal annealing temperature, up to which the sheet resistivity remained stable.

* Corresponding author.
E-mail address: mkozubal@ite.waw.pl (M.A. Kozubal).

http://dx.doi.org/10.1016/j.mssp.2017.10.016
Received 8 June 2017; Received in revised form 13 October 2017; Accepted 15 October 2017
1369-8001/ © 2017 Elsevier Ltd. All rights reserved.

Hydrogen implant isolation was chosen instead of the standard QCL processing involving mesa etching, as it offers a series of benefits. It reduces number of technological steps significantly, from 25 to 14 in our case. Furthermore, it allows for a construction that results in better heat dissipation. Proton implantation isolation offers a good precision in controlling the depth of a modified material, up to even tens of micrometres when using highly energetic protons. Main challenges are the choice of masking layer that effectively stops the highly energetic ions and the lateral isolation under the stripes of masking layer. The implantation method, combined with masking for area-selective modification, proves to be superior to the mesa etching. It is very efficient in planar technologies, thus serving as a powerful tool in ICs and laser structures manufacturing.

2. Simulations of ion implantation

In this section we described the planning steps for establishing the optimal conditions for the hydrogen implant isolation, which led to the choice of the ion energy and type of masking layer. They employed the simulations of distributions of implanted protons and vacancies, formed after the irradiation into the GaAs, AlGaAs/GaAs QCL and different types of masking layers. The profiles were calculated from the data simulated by the TRansport in Matter code (TRIM) [21]. Different energies of ions were tested to choose the one that will ensure the proper isolation of the whole 6.2 μm of the active region of the laser. Masking layer was chosen according to its ability to stop the ions and the precision of its processing (pattern definition). The dose used for presented simulations, 1×10^{15} cm^{-2}, was chosen based on the results of electrical measurements.

2.1. Energy choice

We calculated the longitudinal (depth) and lateral distributions of hydrogen and vacancies for the implantation with H^+ ions into the QCL structure. Three energies were considered: 540 keV, 640 keV and 740 keV. We accounted for the standard 7° angle between the beam direction and the sample. Hence, the lateral distributions are slightly shifted.

The depth distributions of hydrogen and vacancies differ in the region from surface up to the maximum, whereas below the maximum they are almost identical, Fig. 1(a). Whereas for the lateral distributions the discrepancies between the ion and vacancy profiles are negligible, Fig. 1(b).

These simulations were calculated for ions incoming from a single entry point and are common in literature. Nevertheless, they were insufficient for analysis of the lateral straggling of ions. Defects introduced this way can lead to unintentional lateral isolation, which could impair final devices; the minimum stripe width in our case was 15 μm [22]. To analyse this the algorithm for calculating the maps of vacancies was developed. These maps provide better insight into the vacancy distributions and its magnitude, Fig. 2. Each map corresponds to the implantation through a window 6 μm wide. Window length was chosen arbitrarily to be wide enough for the utmost left and right profiles not to overlap during summation. The number of simulated ions was designed to be as high as 10^5, to minimize the statistical noise. Using the TRIM software, we simulated vacancy maps for the implantation where ions enter the material from a single entry point, accommodating the 7° sample tilt. Then we consecutively shifted the original profile 40 times in lateral direction by 150 nm and summed all of them (40 × 150 nm = 6 μm). This overall distribution was subsequently smoothened with 2D Gaussian filter (σ = 1) and the data below 3 orders of magnitude from the maximum were cut, both as insignificant and to remove background noise.

Whenever the ions enter the material through a defined opening in a mask, they undergo lateral straggling introducing the vacancies under the masked areas, as shown in Fig. 2. This effect is most significant near

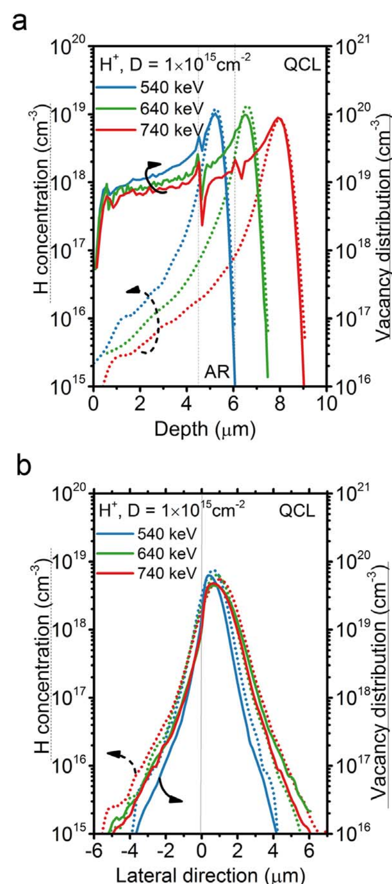

Fig. 1. Simulations of (a) longitudinal (depth) and (b) lateral distributions of hydrogen (left axis, dashed lines) and vacancies (right axis, solid lines). The target was QCL with the $Al_{0.45}Ga_{0.55}As$ / GaAs active region (denoted as AR), after the proton implantation with three different energies and an arbitrary fluency of 1×10^{15} cm^{-2}. Lateral profile (b) accounted for the 7° tilt angle.

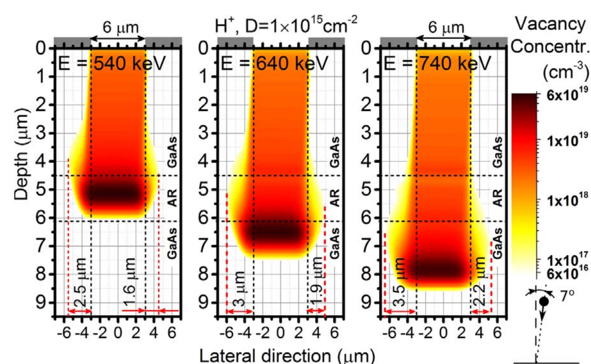

Fig. 2. Maps of vacancies in the QCL sample with $Al_{0.45}Ga_{0.55}As$/GaAs active region (denoted as AR) formed by the proton implantation at energies of 540 keV, 640 keV or 740 keV to a fluency of 1×10^{15} cm^{-2} at the 7° to the normal to the sample's surface. Ions were impinging from a window in a masking layer of arbitrary length of 6 μm.

the maximum of the depth distribution. The lateral profiles extend beyond the mask's edge up to 4.1 μm, 4.9 μm and 5.7 μm in total for the energies of 540 keV, 640 keV and 740 keV, respectively.

The vacancy maps presented are for the asymmetrical situation, as there are two extreme configurations of mask and ion beam possible. The plane of ion beam direction and normal to the surface can either be parallel or perpendicular to the planes defined by the mask's edges. The former leads to symmetrical profiles while the later to asymmetrical ones, as presented in Fig. 2.

With higher ion energy both the maximum of atom concentration

Download English Version:

https://daneshyari.com/en/article/7118149

Download Persian Version:

https://daneshyari.com/article/7118149

Daneshyari.com